Electronic Supplementary Material (ESI) for Analyst.

^{19}F NMR Enantiodiscrimination and Diastereomeric Purity Determination of Amino Acids, Dipeptides, and Amines

Lihua Xu[a], Qiong Wang[b], Yan Liu[d], Songsen Fu[a]*, Yufen Zhao[a][c][d], Shaohua Huang[a]*, Biling Huang[a]*

[a] Institute of Drug Discovery Technology, Ningbo University, Ningbo, 315211, P.R. China.

[b] College of Chemistry, Shandong Normal University, Jinan, 250014, P.R. China.

[c] Department of Chemical Biology, College of Chemistry and Chemical Engineering, and the Key Laboratory for Chemical Biology of Fujian Province, Xiamen University, Xiamen, 361005, P.R. China.

[d] Key Lab of Bioorganic Phosphorus Chemistry & Chemical Biology, Department of Chemistry, Tsinghua University, Beijing, 100084, P.R. China.

Corresponding author: *Biling Huang, huangbiling@nbu.edu.cn, ORCID: 0000-0002-1060-8787; *Shaohua Huang, huangshaohua@nbu.edu.cn; *Songsen Fu, fusongsen@nbu.edu.cn.

Supporting Information

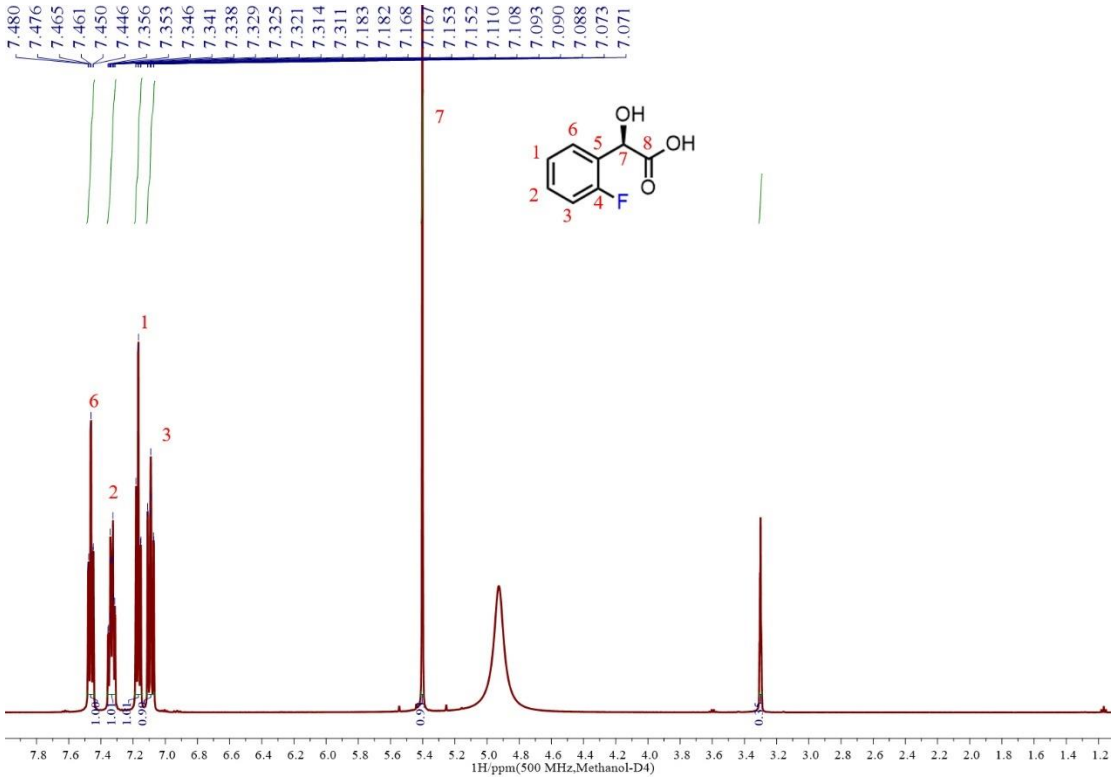

Figure S1. ^{1}H NMR spectrum of (*R*)-2FHA (in MeOH-d_4). ^{1}H NMR: 7.462 ppm (td, 1H, $^{3}J_{H\text{-}H}$ 7.44Hz, $^{4}J_{H\text{-}H}$ 1.68 Hz, CH), 7.333 ppm (m, 1H, CH), 7.167 ppm (td, 1H, $^{3}J_{H\text{-}H}$ 7.62 Hz, $^{4}J_{H\text{-}H}$, 0.95 Hz, CH), 7.091 ppm (m, 1H, CH), 5.402 ppm (s, 1H, OH-C<u>H</u>-COOH).

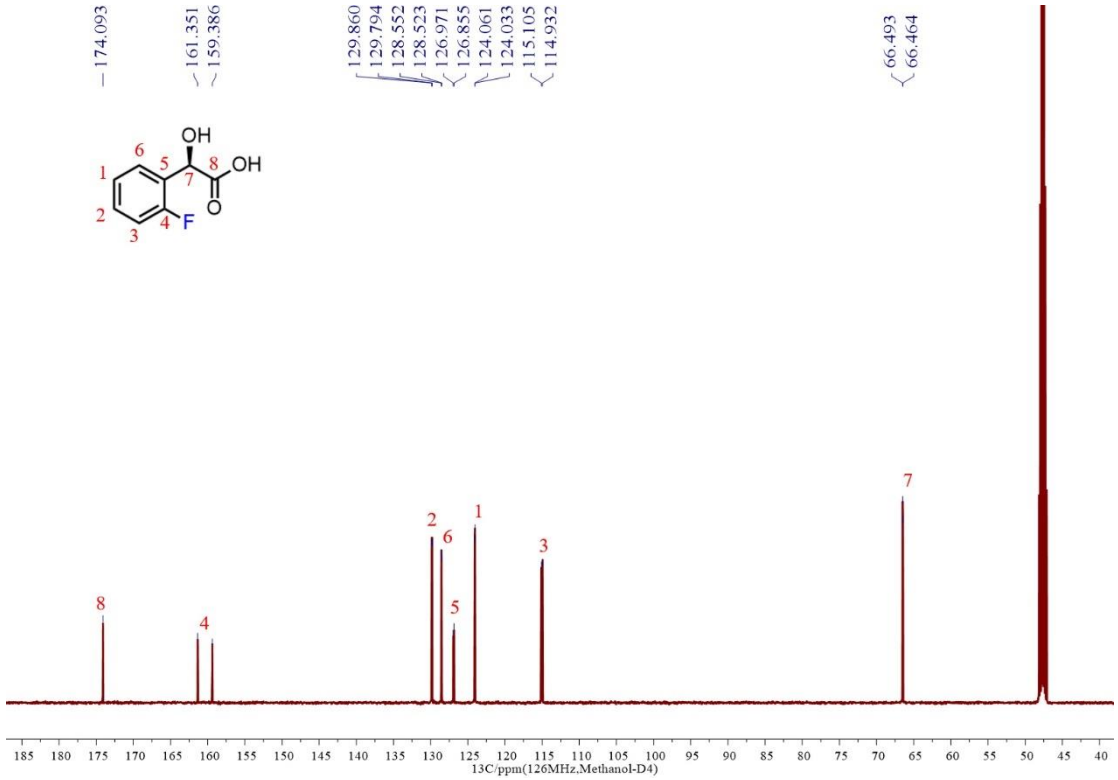

Figure S2. ^{13}C NMR spectrum of (*R*)-2FHA (in MeOH-d_4). ^{13}C NMR: 174.077 ppm (s, COOH), 162.314 ppm (d, $^{1}J_{C\text{-}F}$, 247.12 Hz, CHF), 129.816 ppm (d, $^{3}J_{C\text{-}F}$, 8.94 Hz, CH), 128.525 ppm (d, $^{3}J_{C\text{-}F}$, 3.73 Hz, CH), 126.895 ppm (d, $^{2}J_{C\text{-}F}$, 14.56 Hz, CH-C-CHF), 124.038ppm (d, $^{4}J_{C\text{-}F}$ 3.52 Hz, CH), 115.00 ppm (d, $^{2}J_{C\text{-}F}$, 21.56 Hz, CH), 66.471 ppm (d, $^{3}J_{C\text{-}F}$, 3.57 Hz, C-CH-COOH).

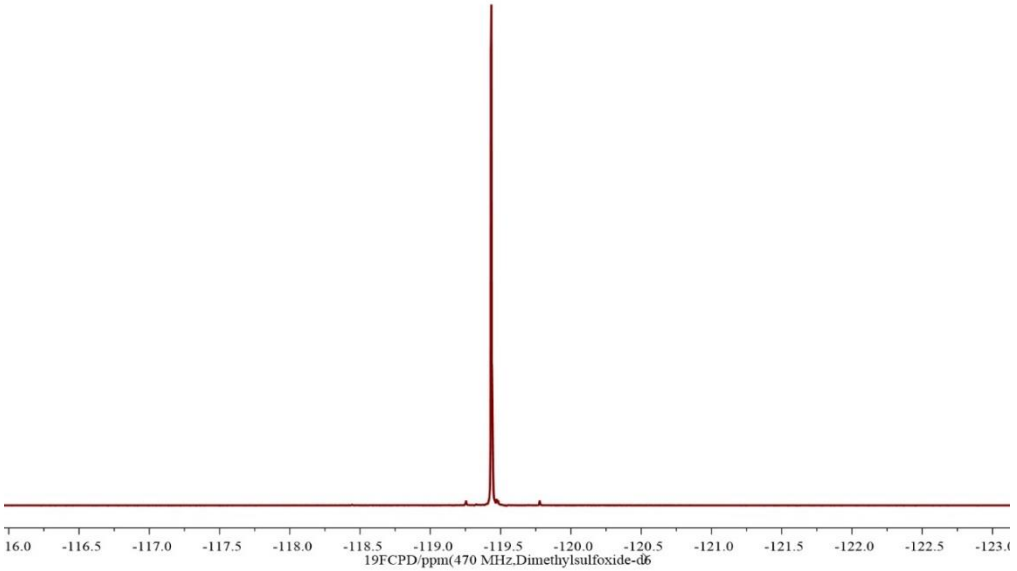

Figure S3. ^{19}F NMR spectrum (decoupling with ^{1}H nuclei) of (*R*)-2FHA (in DMSO-d_6).

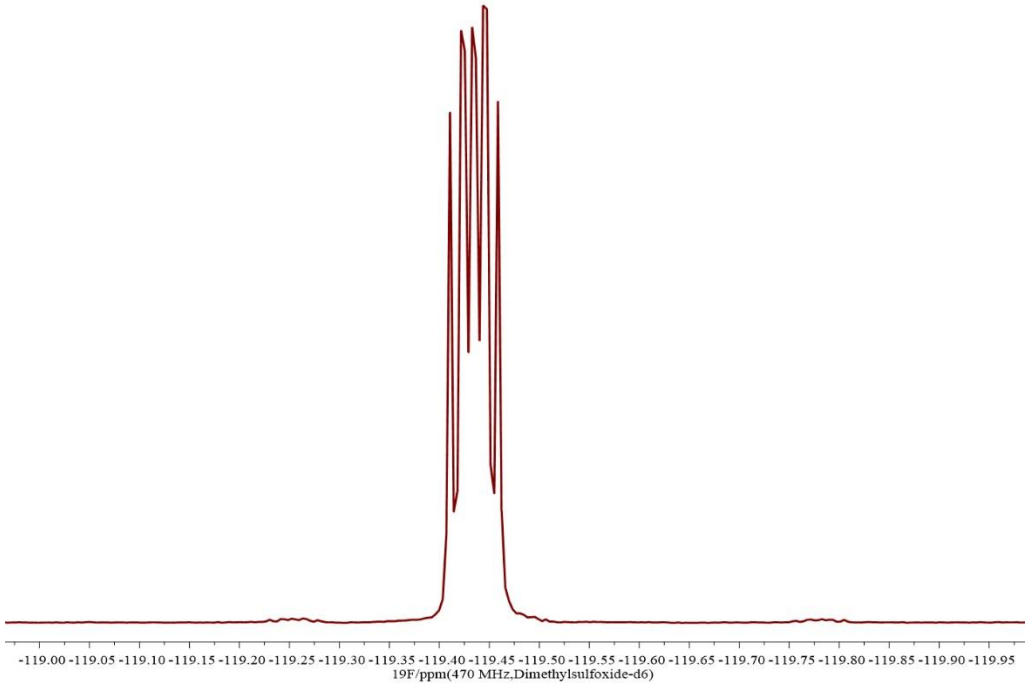

Figure S4. ^{19}F NMR spectrum (coupling with ^{1}H nuclei) of (*R*)-2FHA (in DMSO-d_6).

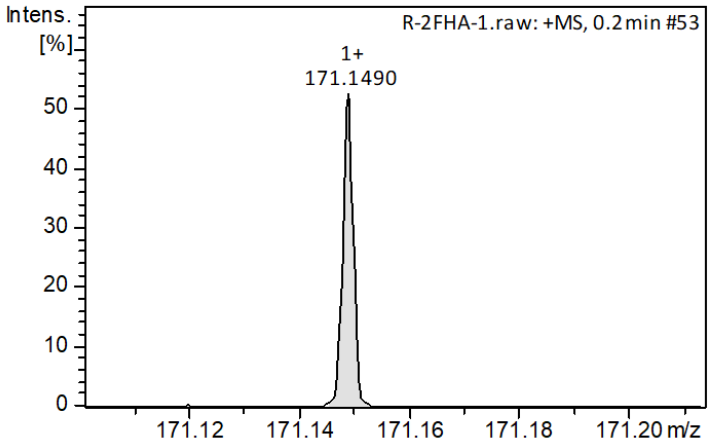

Figure S5. High-resolution ESI-MS (HRMS) analysis of the (*R*)-2FHA. HRMS: 171.1474 (calculated $[M+H]^+$), 171.1490 (observed $[M+H]^+$).

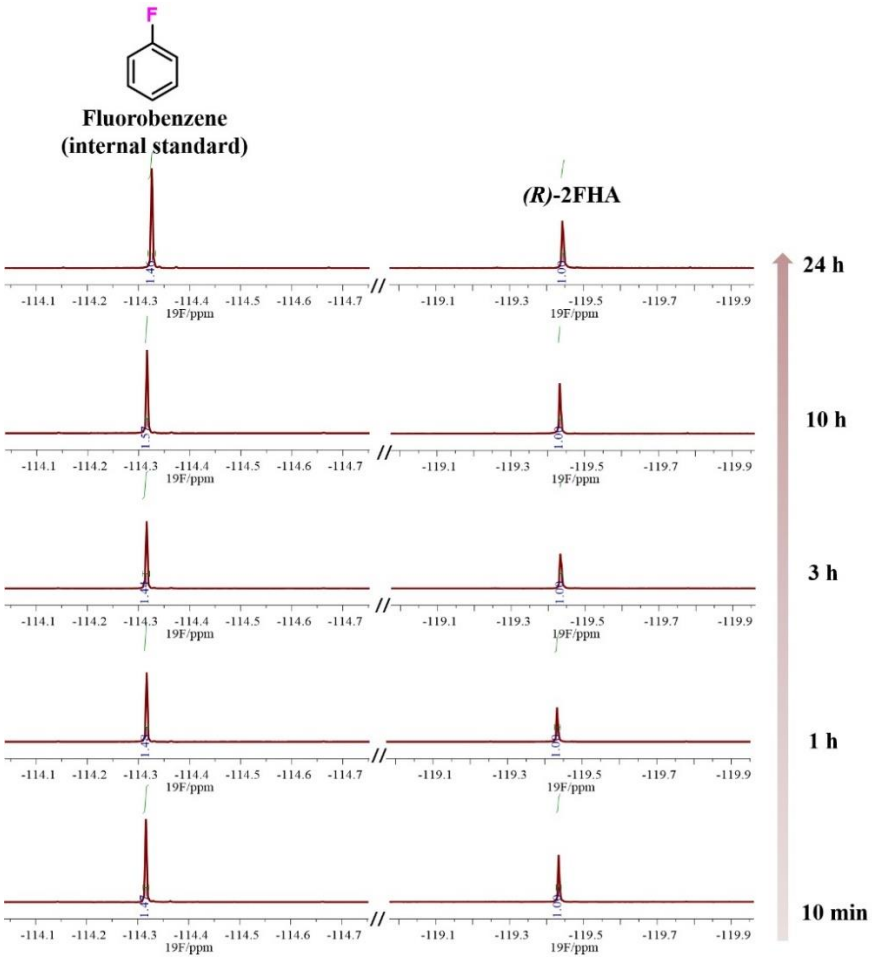

Figure S6. Stability of (*R*)-2FHA in EtOH (20 mM) monitored by ^{19}F NMR spectroscopy. Fluorobenzene (30 mM) was used as an internal standard for integral analysis of ^{19}F resonance signal of (*R*)-2FHA over time.

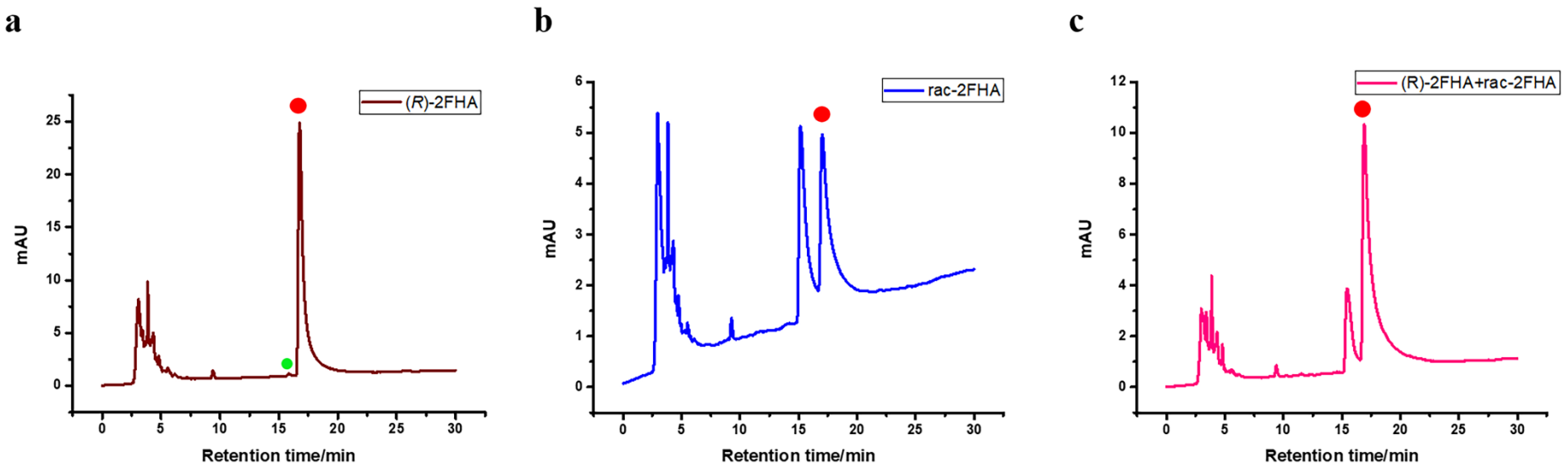

Figure S7. The chromatograms of (a) (*R*)-2FHA, (b) racemic 2FHA, and (c) (*R*)-2FHA mixing with racemic 2FHA analyzed by reverse phase chiral HPLC. The *red* dots labeled peak indicates (*R*)-2FHA. The *green* dot labeled peak possibly represents (*S*)-2FHA, its relative proportion to (*R*)-2FHA (99.463%) is 0.537%.

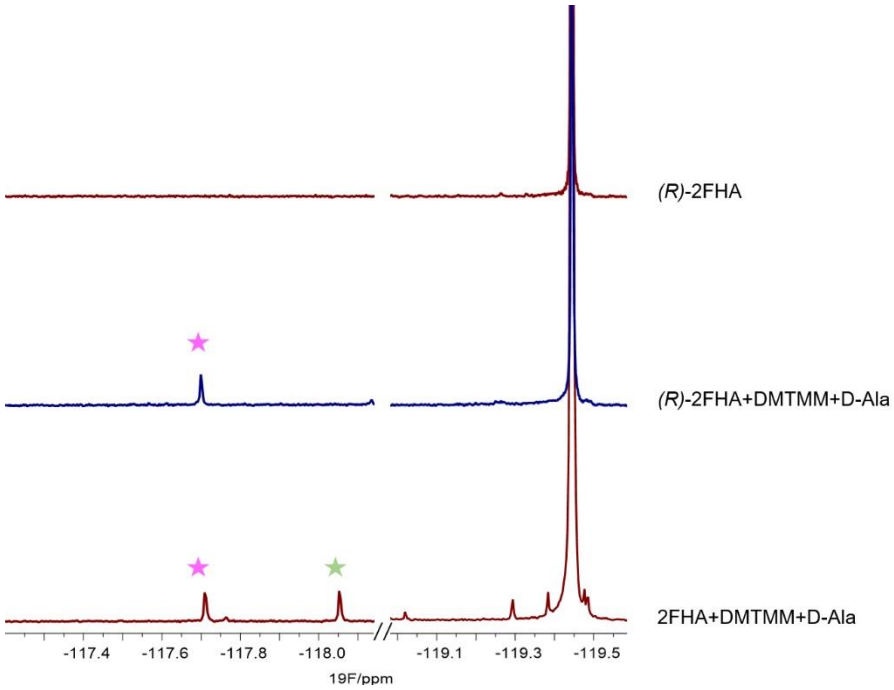

Figure S8. D-Ala was modified by (*R*)-2FHA and *rac*-2FHA. The newly emerged *red* pentacle labeled peaks and *green* pentacle labeled (*red* pentacle labeled) were respectively unambiguously assigned as the resultant derivative (*R*)-2FHA-D-Ala and (*S*)-2FHA-D-Ala.

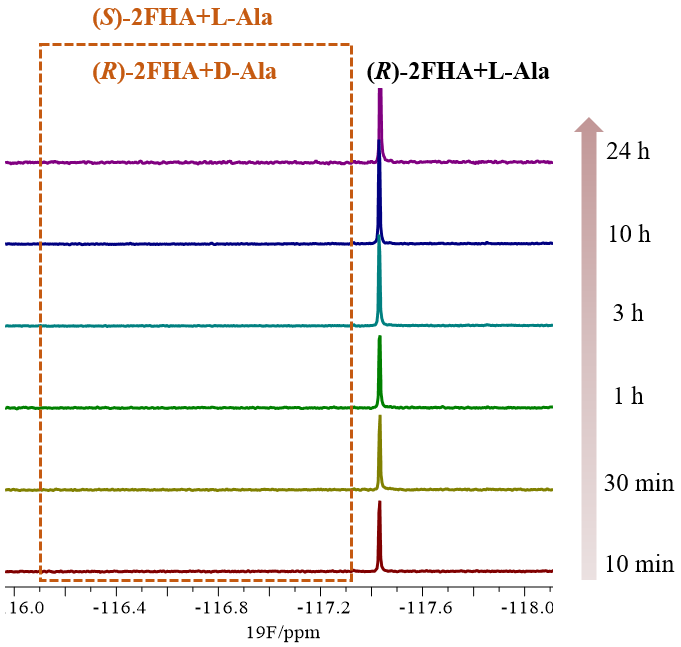

Figure S9. Stacked ^{19}F NMR spectra of (*R*)-2FHA-L-Ala over reaction time. The *orange* box labeled the region indicates the peak of (*S*)-2FHA-L-Ala, which corresponds to its mirror-image (*R*)-2FHA-D-Ala.

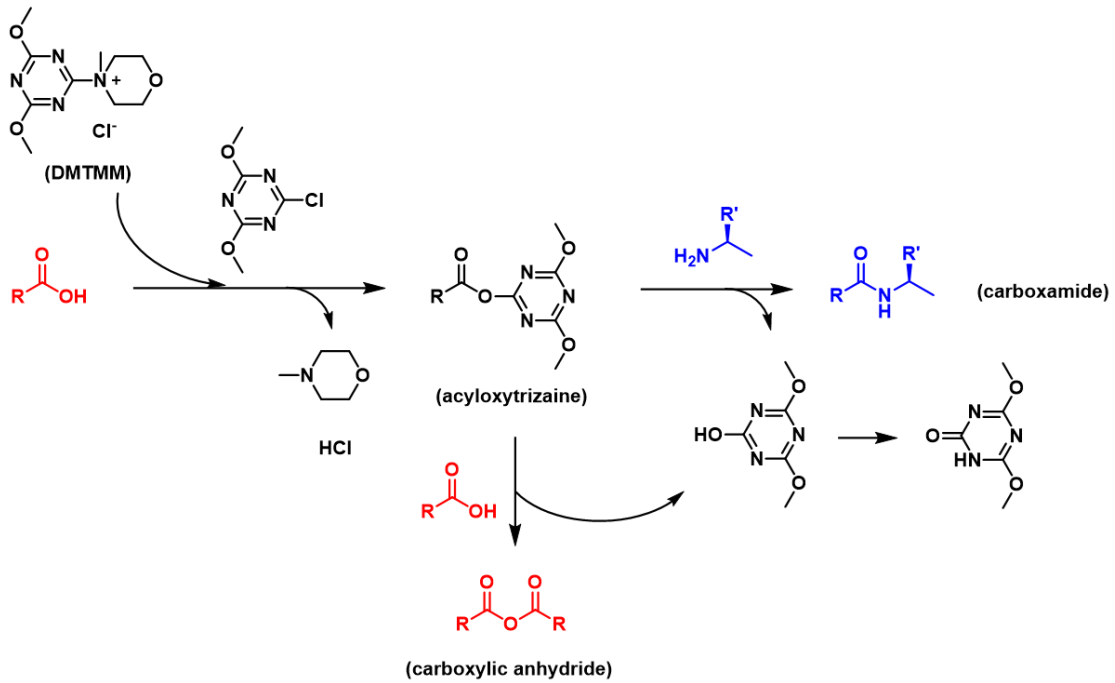

Figure S10. Mechanism of condensation reaction mediated by DMTMM.

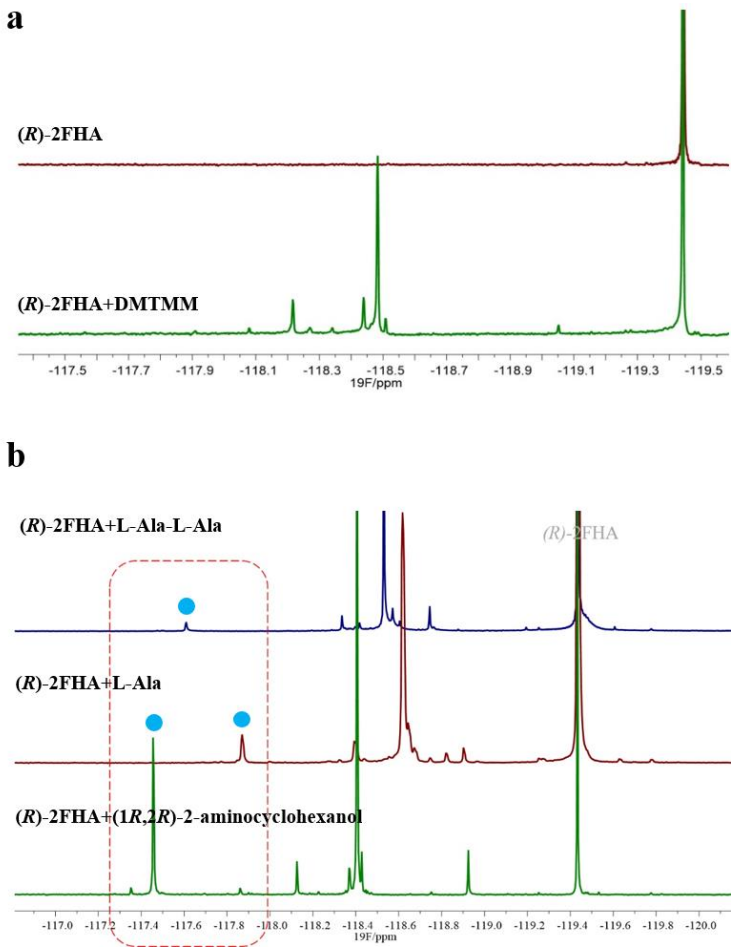

Figure S11. Full ^{19}F NMR spectra of (a) (*R*)-2FHA and (*R*)-2FHA treatment with DMTMM. (b) Stacked full ^{19}F NMR spectra of (*R*)-2FHA labelling L-Ala-L-Ala, L-Ala, and (1*R*,2*R*)-2-aminocyclohexanol. The *sky-blue* dot labeled peaks represented the target products.

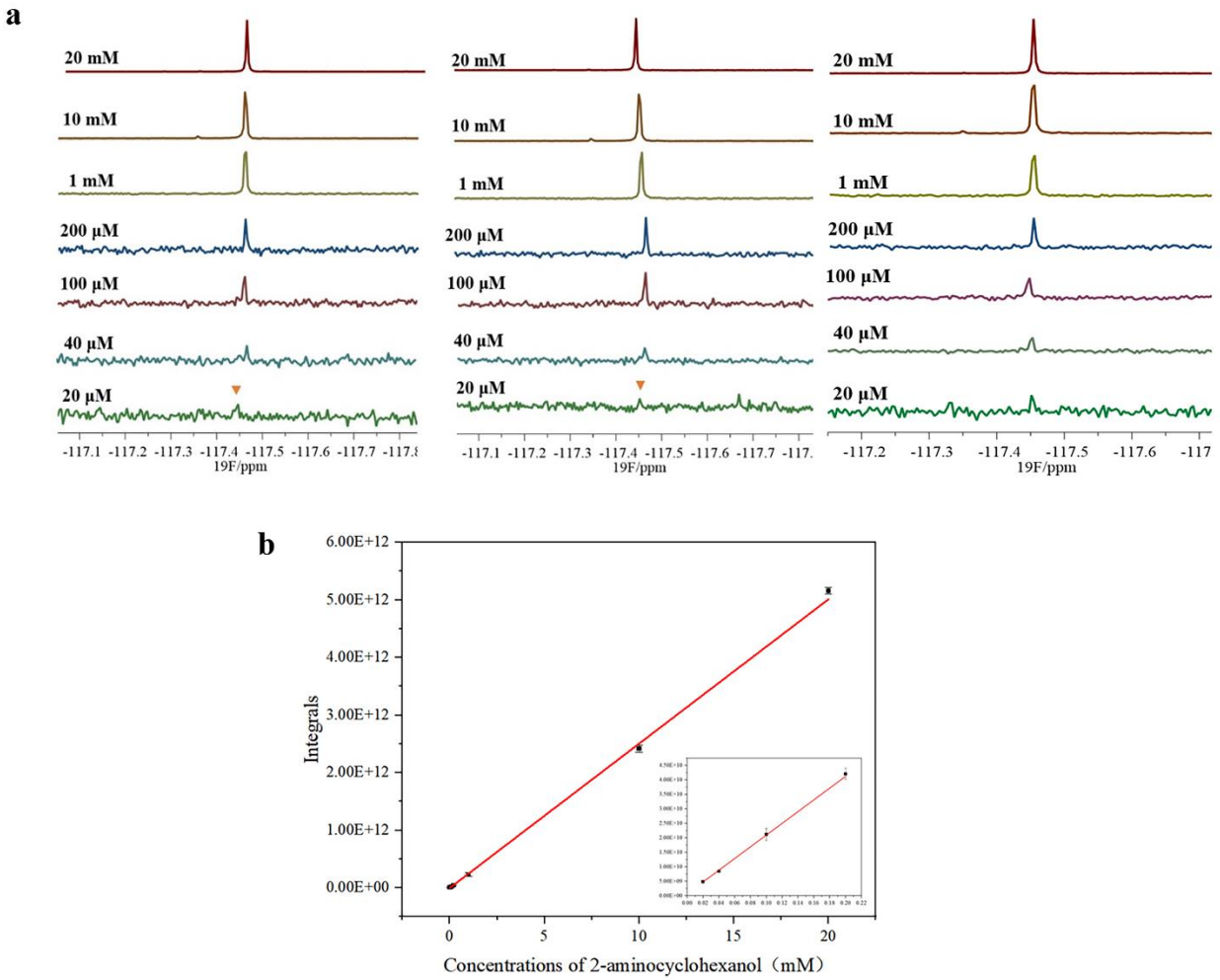

Figure S12. Limit of detection of (*1R,2R*)-2-aminocyclohexanol ((*1R,2R*)-***f***) measured by (*R*)-2FHA. (a) Superimpositions of the ^{19}F NMR

spectra of (*R*)-2FHA labelling different concentrations of (*1R,2R*)-***f*** (20 μM, 40 μM, 100 μM, 200 μM, 1 mM, 10 mM, 20 mM). Three stacked spectra represent the independent triplicated experiments. (b) The integrals of ^{19}F NMR (512 scans) signals of (*R*)-2FHA-(*1R,2R*)-***f*** change with the increase in concentrations of (*1R,2R*)-***f*** (y=2.024E11x+7.41E8, R^2=0.997). The error bars were calculated from the three triplicated experiments. The embedded figure was amplified from the region between 20 μM and 1 mM.

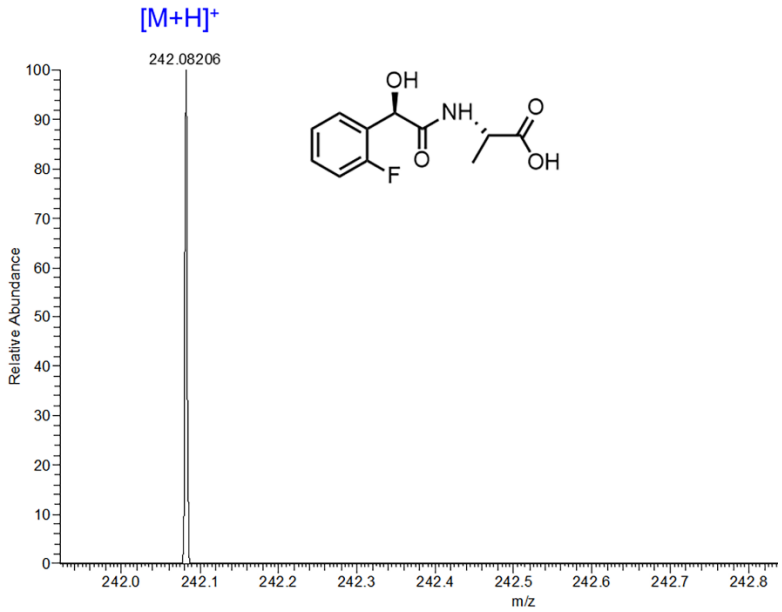

Figure S13. High-resolution ESI-MS (HRMS) analysis of the derivative (*R*)-2FHA-D-Ala. HRMS: 242.0821 (calculated $[M+H]^+$), 242.0820 (observed $[M+H]^+$).

Table S1. Biogenic amino acids discussed in this work. The ^{19}F chemical shifts and $\Delta\Delta\delta(^{19}F)$ values, and enantiodiscrimination factors ($\Delta\Delta\delta$/linewidth) were listed.

Entry	Amine acid	D $\delta(^{19}F)$/ppm	L $\delta(^{19}F)$/ppm	$\Delta\Delta\delta(^{19}F)$/Hz	$\Delta\Delta\delta(^{19}F)$/ppm	D linewidth/Hz	L linewidth/Hz	$\Delta\Delta\delta$/linewidth
1	Gly	-119.076		—	—	2.44		—
2	Ala	-117.699	-117.980	132.247	0.281	4.14	4.02	16.21
3	Arg	-117.554	-118.011	215.077	0.457	4.20	3.37	28.41
4	Asp	-118.007	-118.193	87.556	0.186	4.34	3.32	11.43
5	Asn	-117.841	-118.015	81.889	0.174	3.03	2.84	13.95
6	Cys	-117.767	-118.144	177.427	0.377	4.00	5.46	18.76
7	Gln	-117.691	-117.892	94.596	0.201	4.27	3.02	12.98
8	Glu	-117.661	-117.918	120.951	0.257	3.21	3.21	18.84
9	His	-117.748	-117.879	61.652	0.131	3.75	4.21	7.75
10	Ile	-117.417	-117.767	164.622	0.35	5.80	5.35	14.76
11	Leu	-117.733	-118.159	200.488	0.426	3.61	4.22	25.61
12	Lys	-117.560 -117.827	-117.870 -117.992	$145.895^{(\alpha)}$ $77.653^{(\varepsilon)}$	$0.31^{(\alpha)}$ $0.165^{(\varepsilon)}$	$3.81^{(\alpha)}$ $3.17^{(\varepsilon)}$	$3.14^{(\alpha)}$ $3.14^{(\varepsilon)}$	$20.99^{(\alpha)}$ $12.31^{(\varepsilon)}$
13	Met	-117.621	-117.922	141.659	0.301	2.93	3.83	20.96
14	Phe	-118.052	-118.220	79.083	0.168	3.55	3.66	10.97
15	Pro	-117.572	-117.129	208.533	0.443	1.51	2.12	57.45
16	Ser	-117.793	-117.798	2.353	0.005	4.14	3.94	0.29
17	Thr	-117.493	-117.895	189.193	0.402	3.71	3.53	26.13
18	Trp	-118.118	-118.188	32.944	0.07	2.80	2.80	5.88
19	Val	-117.426	-117.818	184.486	0.392	3.73	4.40	22.69

Table S2. Mirror-image dipeptides analyzed in the current work, the ^{19}F chemical shifts of the resultant derivatives and their $\Delta\Delta\delta(^{19}F)$ values as well as enantioresolution factors were clearly presented.

Dipeptides	DD $\delta(^{19}F)$/ppm	LL $\delta(^{19}F)$/ppm	$\Delta\Delta\delta(^{19}F)$/Hz	$\Delta\Delta\delta(^{19}F)$/ppm	DD linewidth/Hz	LL linewidth/Hz	$\Delta\Delta\delta$/linewidth
Phe-Phe	-117.613	-117.705	43.24	0.092	2.85	2.25	8.48
Ala-Ala	-117.619	-117.881	123.14	0.262	3.58	3.82	16.64
Val-Val	-117.38	-117.652	127.84	0.272	3.39	2.49	21.74
Leu-Leu	-117.69	-118.024	156.98	0.334	5.51	4.66	15.44

Dipeptides	DD $\delta(^{19}F)$/ppm	LL $\delta(^{19}F)$/ppm	DL $\delta(^{19}F)$/ppm	LD $\delta(^{19}F)$/ppm	$\Delta\Delta\delta(^{19}F)$/Hz	$\Delta\Delta\delta(^{19}F)$/ppm	DD linewidth/Hz	LL linewidth/Hz	DL linewidth/Hz	LD linewidth/Hz	$\Delta\Delta\delta$/linewidth
Ser-His	-118.119	-118.263	—	—	67.78	0.144	6.04	5.49	—	—	5.88
Ser-His	—	—	-118.077	-118.158	38.13	0.081	—	—	5.49	4.67	3.75
His-Ser	-118.031	-118.206	—	—	82.38	0.175	7.14	2.20	—	—	8.82
His-Ser	—	—	-118.064	-118.239	82.38	0.175	—	—	6.04	5.49	7.14

Table S3. Chiral non-AAs amines discussed in this work, the ΔΔδ(^{19}F) values and enantioresolution factors were definitely determined.

Entry	Non-AAs amines	D δ(^{19}F)/ppm	L δ(^{19}F)/ppm	ΔΔδ(^{19}F)/Hz	ΔΔδ(^{19}F)/ppm	D linewidth	L linewidth	ΔΔδ/linewidth
a	2-aminooctane	-117.760	-117.765	2.35	0.005	—	—	—
b	3-aminoheptane	-117.667	-117.772	49.35	0.105	2.41	3.04	9.06
c	2-aminobutane	-117.637	-117.747	51.7	0.11	2.83	3.60	8.04
d	1,2-dimethylpropylamine	-117.572	-117.751	84.13	0.179	2.51	2.20	17.86
e	1-methoxy-2-propylamine	-117.675	-117.762	40.89	0.087	2.19	2.83	8.15
f	2-aminocyclohexanol	-117.446	-117.846	188	0.4	4.04	3.79	24.01
g	valinol	-117.486	-117.957	221.37	0.471	2.67	2.67	41.46
h	1-aminoindan	-117.467	-117.592	58.75	0.125	4.06	3.75	7.52
i	phenylalaninol	-117.877	-117.892	7.05	0.015	2.36	2.36	1.49
j	α-methylbenzylamine	-117.672	-117.695	10.81	0.023	2.35	2.82	2.09

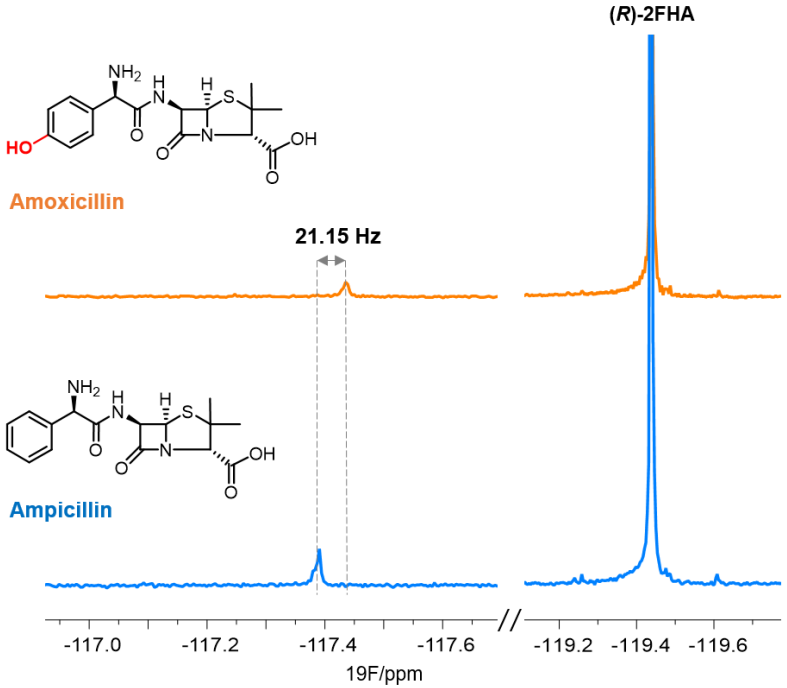

Figure S14. Discrimination of the antibiotics amoxicillin and ampicillin by (*R*)-TFHA. The difference of ^{19}F chemical shifts between (*R*)-TFHA labeled amoxicillin and ampicillin was determined to be 21.15 Hz.

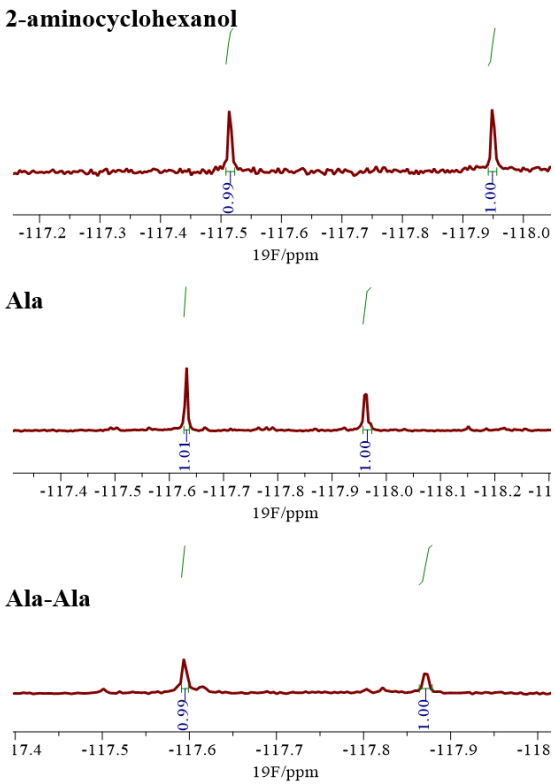

Figure S15. Differentiation of the racemic solutions of 2-aminocyclohexanol (***f***), Ala, and Ala-Ala by (*R*)-2FHA. The integrals of each signal were clearly labeled.

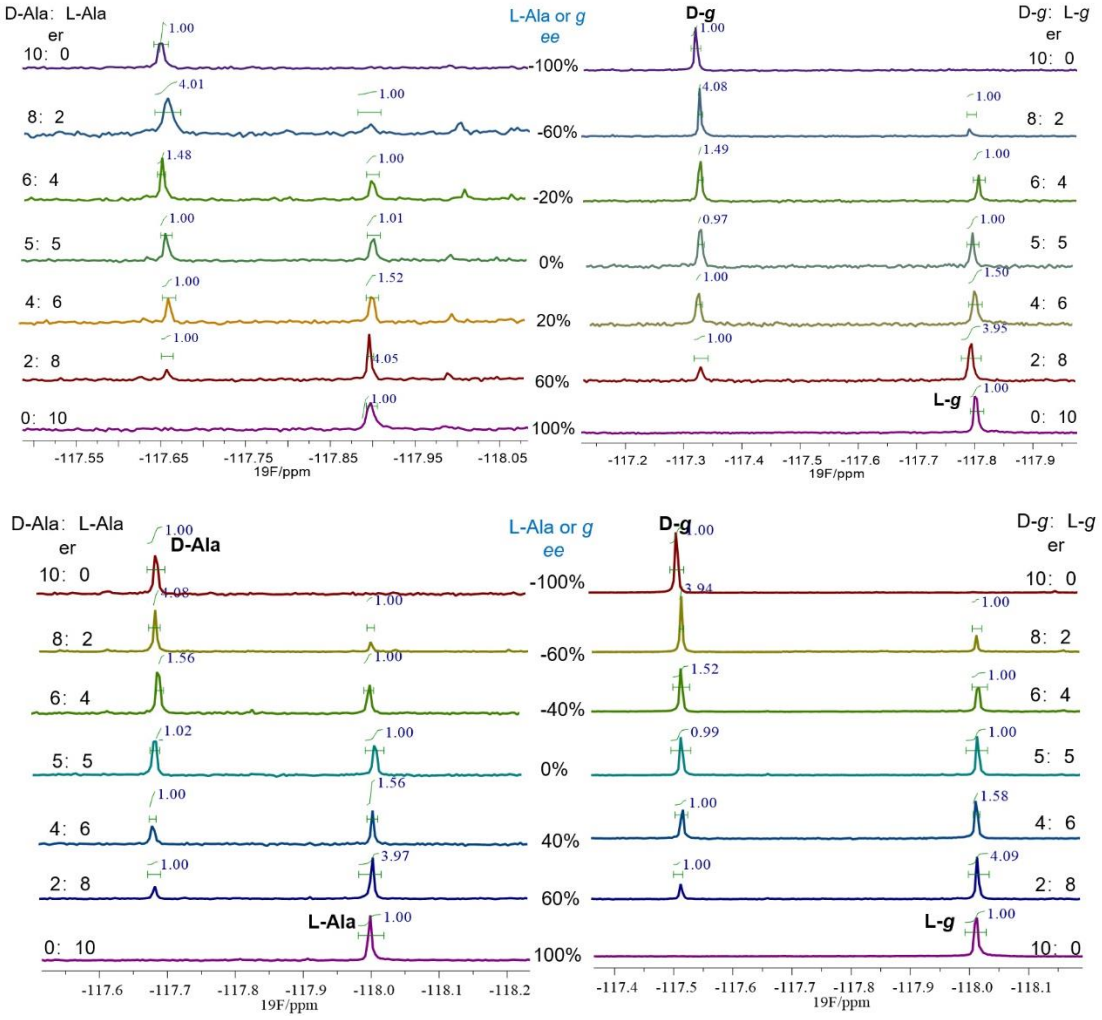
D-Ala: L-Ala
er
10: 0
8: 2
6: 4
5: 5
4: 6
2: 8
0: 10
L-Ala or g
ee
-100%
-60%
-20%
0%
20%
60%
100%
D-g
D-g: L-g
er
10: 0
8: 2
6: 4
5: 5
4: 6
2: 8
L-g
0: 10
19F/ppm
D-Ala
L-Ala
40%
-40%

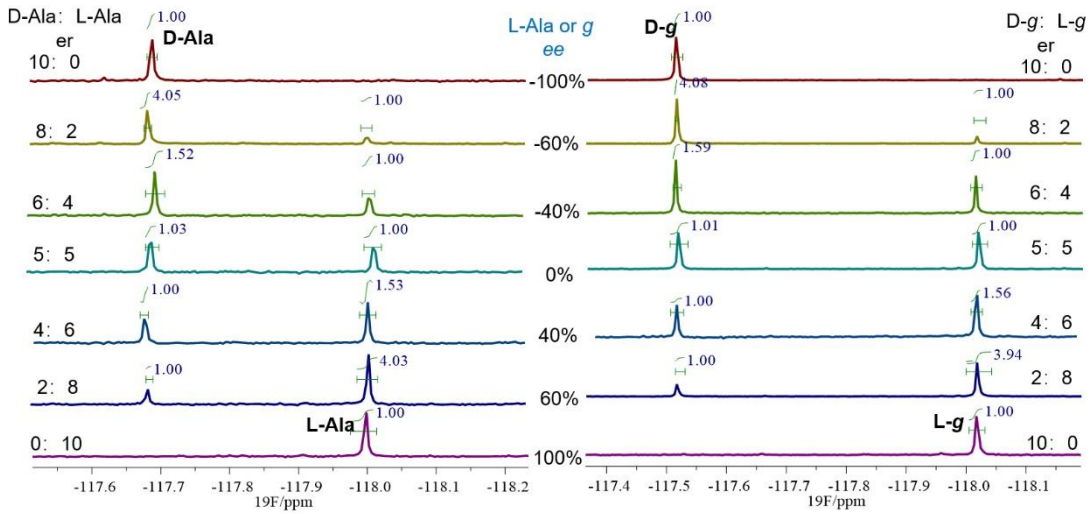

Figure S16. Determination of *ee* values of L-Ala or D-valinol (D-***g***) in nonracemic solutions (the independent triplicated experiments). The relative ^{19}F integrals (D-Ala *versus* L-Ala, D-***g*** *versus* L-***g***) in a spectrum were clearly shown (^{19}F NMR: EtOH with 10% (v/v) DMSO-d_6; transmitter frequency 470.63 MHz; 64 scans.)

Table S4. Determination of *de* and *dr* values of L-Ala or D-valinol (D-***g***) in the non-racemic solutions. The calculated *de* and *dr* by the integrals of ^{19}F resonance signals were clearly presented, and SD represents the error on each *de* or *dr* value. The *de*, *dr* and SD values were obtained from the independent triplicated experiments.

	ee **(%,by theoretical)**	***er*** **(%,by theoretical)**	***de*** **(%,by NMR)**	**SD (%)**	***dr*** **(%,by NMR)**	**SD (%)**
L-Ala	100	10	100	0	10	0
			100		10	
			100		10	
	60	4	60.08	0.27	4.01	0.03
			60.62		4.08	
			60.39		4.05	
	20	1.5	19.35	1.26	1.48	0.04
			20.63		1.52	
			21.87		1.56	
	0	1	-0.49	1.02	0.99	0.02
			0.99		1.02	
			1.47		1.03	
	-20	0.67	-20.63	0.47	0.66	0.01
			-21.56		0.64	
			-20.94		0.65	
	-60	0.25	-60.40	0.66	0.25	0.01
			-61.16		0.24	
			-59.84		0.25	
	-100	0	-100	0	0	0
			-100		0	
			-100		0	

	ee **(%,by theoretical)**	***er*** **(%,by theoretical)**	***de*** **(%,by NMR)**	**SD (%)**	***dr*** **(%,by NMR)**	**SD (%)**
D-*g*	100	10	100	0	10	0
			100		10	
			100		10	
	60	4	60.63	0.64	4.08	0.08
			60.62		4.08	
			59.51		3.94	
	20	1.5	19.68	1.58	1.49	0.05
			20.63		1.52	
			22.77		1.59	
	0	1	1.52	0.59	0.97	0.02
			0.50		0.99	
			0.49		1.01	
	-20	0.67	-20	1.29	0.67	0.02
			-21.87		0.64	
			-22.48		0.63	
	-60	0.25	-59.59	1.23	0.25	0.01
			-61.31		0.24	
			-58.93		0.25	
	-100	0	-100	0	0	0
			-100		0	
			-100		0	

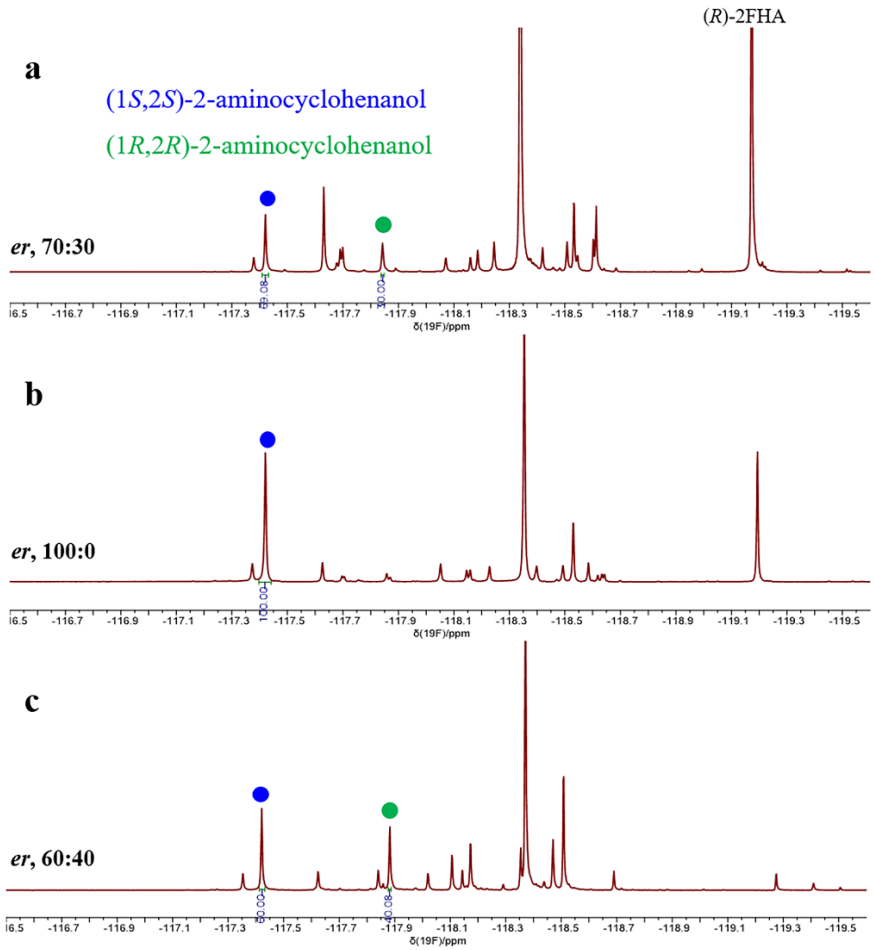

Figure S17. Determination of *dr* of 2-aminocyclohexanol (*f*) in the complex mixtures at different concentrations. The blue and red dots labeled peaks indicate (*R*)-2FHA-(1*S*,2*S*)-2-aminocyclohenanol and (*R*)-2FHA-(1*R*,2*R*)-2-aminocyclohenanol. The integrals of their 19F NMR resonance signals were display.

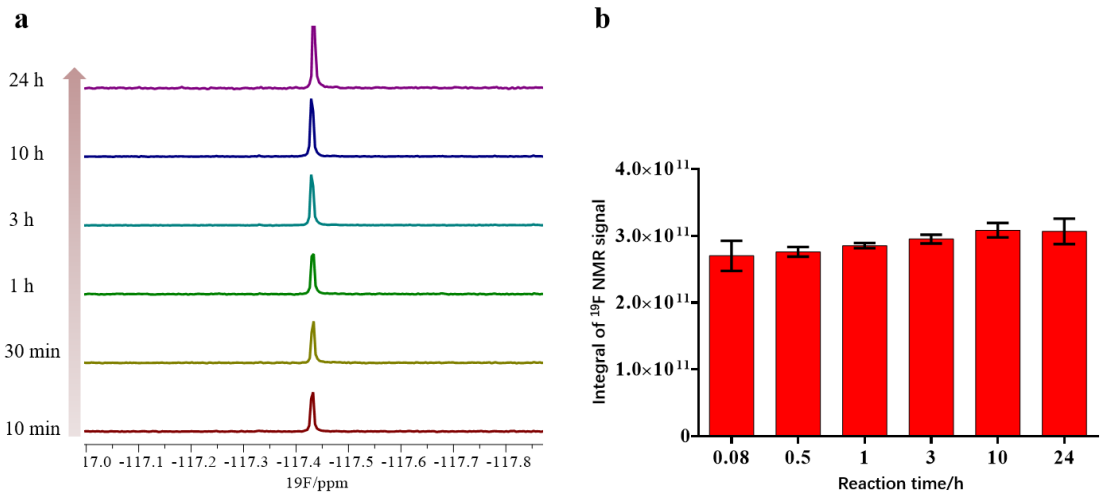

Figure S18. Monitoring the ^{19}F NMR signal intensity of the resultant derivative (*R*)-2FHA-L-Ala. (a) Stacked ^{19}F NMR spectra of (*R*)-2FHA-L-Ala over reaction time. (b) Histogram of integral of ^{19}F NMR signal of (*R*)-2FHA-L-Ala *versus* reaction time.